

A photograph of two women in a modern office setting. The woman on the left, with dark curly hair, is wearing a black sleeveless top and a gold chain necklace. She is holding a white tablet. The woman on the right, with dark hair pulled back, is wearing a grey tank top and a dark blue cardigan. Both women are smiling and looking at the tablet. The background shows a concrete wall and a window with bright light.

Bright ideas for you

At Shell Polymers, we're dedicated to helping our customers create a stronger polyethylene supply chain. That's why we're reimagining the polyethylene industry with our state-of-the-art plant technologies and trusted, tested industry experts. This commitment to offering an unrivaled customer experience by streamlining your supply chain is just one way we **Break the Mold.**

SHELL POLYMERS
MAKING THE EXPERIENCE MATTER

[Click here to learn more
about Shell Polymers](#)

ARTICLE

Centrifugally spun carbon fibers prepared from aqueous poly(vinylpyrrolidone) solutions as binder-free anodes in lithium-ion batteries

Roberto Orrostieta Chavez¹ | Timothy P. Lodge² | Juan Huitron¹ |
Mircea Chipara³ | Mataz Alcoutlabi¹

¹Department of Mechanical Engineering, University of Texas, Edinburg, Texas, USA

²Department of Chemical Engineering and Materials Science and Department of Chemistry, University of Minnesota, Minneapolis, Minnesota, USA

³Department of Physics and Astronomy, The University of Texas Rio Grande Valley, Edinburg, Texas, USA

Correspondence

Mataz Alcoutlabi, Department of Mechanical Engineering, University of Texas, Rio Grande Valley, Edinburg, TX 78539.

Email: mataz.alcoutlabi@utrgv.edu

Abstract

Aqueous solutions of poly(vinylpyrrolidone) (PVP) of various concentrations (20, 25, and 28 wt%) were successfully spun into fibers by centrifugal spinning. The pristine PVP fibers were annealed and carbonized to produce flexible carbon fibers for use as binder-free anodes in lithium-ion batteries. These flexible carbon fibers were prepared by developing a novel three-step heat treatment to reduce the residual stresses in the pristine PVP precursor fibers, and to prevent fiber degradation during carbonization. The thermogravimetric analysis data showed that the annealed fibers yielded a residual mass percentage of 36.0% while the pristine PVP fibers suffered a higher mass loss and only retained 26.5% of original mass above 450 °C (under nitrogen). The electrochemical performance of the carbon-fiber anodes was evaluated by conducting galvanostatic charge/discharge, rate performance, and cycle voltammetry experiments. The 20, 25, and 28 wt% derived binder-free anodes delivered specific charge capacities of 205, 189, and 275 mAh g⁻¹, respectively, after the first cycle at a current density of 100 mA g⁻¹. The results obtained in this work indicate that a feasible pathway towards a large-scale production of carbon-fiber anodes from a 100% aqueous solution can be achieved via centrifugal spinning and subsequent heat treatment.

KEYWORDS

batteries and fuel cells, electrochemistry, thermal properties

1 | INTRODUCTION

Composite materials have enabled engineers to pursue technologies otherwise limited by material performance. Substantial improvements of material properties (e.g., mechanical, thermal, electrical, etc.) can be achieved by the addition of fillers in polymer matrices.¹ Due to their high surface area to volume ratio, composite nanofibers have been extensively used in many applications, such as biomedical, filtration, tissue engineering, and energy

storage.^{2–5} In particular, carbon fibers, and nanofibers prepared by electrospinning and subsequent heat treatment of polymer-fiber precursors have been widely used in energy storage applications.⁶ The carbon phase in these carbon fibers (CFs) can be either amorphous or graphitic, depending on the heat treatment performed during the carbonization/calcination process. Graphite has been the only commercially available anode material for lithium ion batteries (LIBs) due to its low working potential, long cycle life, and low cost. However, the low theoretical

capacity of the graphite anode (372 mAh g^{-1}) fails to satisfy the increasing demand of high performance LIBs for energy storage applications, and in particular for hybrid and electric vehicles.⁷ Li-alloys embedded in flexible CFs with amorphous carbon can be directly used as binder-free anodes in LIBs. The flexible amorphous carbon phase can buffer the volume change of the Li-alloy phase.⁷ In addition, amorphous carbon fibers with many structural defects can accommodate more Li^+ than the ordered lattice in graphite.⁸ Composite CFs can be prepared by various spinning methods applied to a polymer precursor solution containing ceramic and/or metallic fillers, and can be directly used as anode materials in LIBs with improved electrochemical performance such as rapid Li^+ diffusion, long cycle life, and high specific capacity. Currently, polyvinylpyrrolidone (PVP), polyvinyl alcohol (PVA), and polyacrylonitrile (PAN) are the most used polymer precursors to produce carbon fibers for LIB applications.⁹

PAN is the most exploited polymer to produce CFs due to its high melting point and high carbon yield of $<80\%$.^{10,11} In a recent work, PAN-derived CF anodes delivered a steady charge capacity (Li-deinsertion) of 297 mAh g^{-1} after 100 cycles at 100 mA g^{-1} .^{12,13} Unfortunately, PAN has a high cost¹⁴ and the most frequently used solvent dimethylformamide (DMF) has rising health concerns.¹⁵ However, the demand for CFs is increasing. Therefore, researchers and industry have turned their attention to less hazardous and more environmentally benign alternatives, such as PVP and PVA precursor fibers. Both PVP and PVA, in contrast to PAN, are water-soluble and have been recently used in energy storage applications,^{11,15,16,17,18,19}. PVP, particularly, is considered a potential carbon precursor alternative to produce CF anodes due to its low cost. For example, electrospun CFs derived from PVP delivered a reversible specific capacity as high as 450 mAh g^{-1} at the 100th cycle.¹¹ Moreover, high production rates of PVP fibers have been achieved via centrifugal spinning of PVP/ethanol solutions.^{17,18} There have also been successful studies to prepare composite CFs derived from aqueous PVA solutions. For example, centrifugally spun Si/C composite-fiber anodes prepared by centrifugal spinning of aqueous Si/PVA precursor solutions and subsequent heat treatment delivered a steady capacity of 758 mAh g^{-1} after 50 cycles, while PVA-derived CFs delivered 178 mAh g^{-1} .¹⁶ Similarly, Si/C composite nanofibers were prepared by electrospinning of aqueous Si/PVA solutions and subsequent heat treatment for use as a binder-free anode in LIBs. In that work, the Si/C composite nanofibers were enclosed in folded graphene to constrain the volume expansion of the anode after repeated charge/discharge cycles. Because of their improved mechanical properties, the Si/C composite

nanofibers delivered a stable specific capacity of 1191 mAh g^{-1} after 200 cycles at a current density of 1 A g^{-1} .¹⁵ Although the centrifugally spun PVA fibers had smaller diameters than those derived from aqueous PVP solutions, the lower fiber yield of aqueous PVA solutions during centrifugal spinning is a challenge for the adoption of PVA-based carbon fibers at a large-scale production.

PVP, on the other hand, has a much higher fiber yield than PVA during centrifugal spinning. Nonetheless, to the best of our knowledge, there have not been studies on the use of centrifugally spun CFs derived from aqueous PVP precursor solutions for use as anodes for LIBs. Moreover, hematite $\alpha\text{-Fe}_2\text{O}_3$ fibers were prepared by centrifugal spinning of aqueous $\text{PVP/Fe}(\text{NO}_3)_3 \cdot 9\text{H}_2\text{O}$ precursor solutions and subsequent heat treatment to fabricate $\text{Fe}_3\text{O}_4/\text{C}$ composite-fiber anodes for LIBs. The synthesized $\alpha\text{-Fe}_2\text{O}_3$ fibers had a hollow multiwalled structure with wall thickness of $55 \pm 15 \text{ nm}$ and an outer diameter of $850 \pm 90 \text{ nm}$ and were used in PAN/ Fe_3O_4 precursor solution to prepare the $\text{Fe}_3\text{O}_4/\text{C}$ composite fibers.²⁰ The $\text{Fe}_3\text{O}_4/\text{C}$ composite-fiber anode delivered a capacity of 505 mAh g^{-1} at the 100th cycle at 100 mA g^{-1} .²⁰

PVP is less commonly used to produce CFs due to its relatively large volume shrinkage after carbonization.²¹ However, it has been shown that the carbon yield from PVP can be increased by adopting a more complex heat treatment.^{10,22} This current study strives to maximize the production of centrifugally spun CFs by optimizing the PVP concentration in aqueous solutions and implementing a novel heat treatment that aims to decrease the large volume shrinkage observed in PVP fibers at higher carbonization temperatures. Centrifugal spinning is an emerging technology used to produce micro/nano fibers at rates of up to 1 g/min on the laboratory scale, compared to a 0.3 g/min rate for a conventional laboratory scale electrospinning setup.²³ Based on the results obtained here, a feasible pathway towards a large-scale production of CFs from a 100% aqueous solution can be achieved via centrifugal spinning and a subsequent three-step heat treatment.

2 | EXPERIMENTAL

2.1 | Material

Poly(vinylpyrrolidone) (PVP) with an average molecular weight (Mw) of 1,300,000 was purchased from Sigma-Aldrich USA. Deionized (DI) water, $18 \text{ M}\Omega \text{ cm}$, was produced in-house (Milli-Q, Millipore Ltd., U.K.). The 1 M LiPF_6 salt and dimethyl carbonate (DMC) were purchased from Alpha Aesar. Ethylene carbonate (EC) was purchased from Sigma Aldrich.

TABLE 1 Spinning parameters for the fabrication of centrifugally spun PVP fibers

Polymer concentration (wt%)	Rotational speed (rpm)	Spinning time (min)	Humidity during successful fiber yield (%)	Fiber formation
10	4000–9000	3–8	N/A	No
15	4000–9000	3–8	N/A	No
20	6000	4	< 40	Yes
25	9000	5	< 60	Yes
28	9000	8	< 60	Yes

Abbreviation: PVP, poly(vinylpyrrolidone).

2.2 | Preparation of carbon fibers

The precursor fibers were prepared from 20 g aqueous solutions with PVP wt% concentrations of 10, 15, 20, 25, and 28. The polymer was dissolved in DI water, and the as-obtained solution was homogenized by magnetic stirring at 70 °C for 5 h. Solutions of 25 wt% and higher concentrations were subjected to an additional 5 h of stirring to achieve complete homogenization. The PVP solutions were then spun in laboratory-scale centrifugal spinning equipment (FiberRio Cyclone L-1000 M). The spinneret was equipped with 30-gauge regular bevel needles (EXELINT, U.S.A). A variety of spinneret rotational speeds and spinning times were explored for each solution concentration. The centrifugal spinning parameters and solution properties used to prepare the PVP fibers are given in Table 1.

The fibers were collected as a mat and subsequently annealed at 150 °C for 24 h, in air (ELF 11/6 Carbolite Gero, UK). The fibers were left in air to reach room temperature and then placed in a tube furnace (OTF-1200X MTI Corporation, US) to be stabilized in air at 270 °C for 4 h (1 °C/min) followed by carbonization under an Argon atmosphere at 700 °C for 3 h (5 °C/min).

2.3 | Characterization

The morphology of the CFs was investigated by scanning electron microscopy (SEM; Sigma VP Carl Zeiss, Germany) coupled with an energy dispersive spectroscopy (EDS) system (EDAX, Mahwah, NJ, USA) to investigate the elemental composition. To determine the average fiber diameter, 300 measurements were taken, 60 per image, across a total of five different SEM images scaled on ImageJ software. Similarly, the histograms were produced using 300 randomly selected measurements. Thermogravimetric analysis (TGA; 209 F3 Tarsus NETZSCH, Germany) was conducted in air and nitrogen atmospheres to investigate the effect of annealing on fiber degradation. Raman spectra of PVP powder and precursor

nanofibers prepared from aqueous PVP solutions of different concentrations (20%, 25%, and 28%) were obtained with a Renishaw InVia confocal spectrometer operating at 785 nm.

2.4 | Electrochemical measurements

The electrochemical performance of carbon-fiber anodes was evaluated using CR2032-type coin cells. CFs with a half-inch diameter were punched out and used directly as binder-free anodes. The CFs was used as the working electrode while a lithium foil was used as the counter electrode. The weight of these anodes ranged between 4–9 mg. The Li-ion half-cells (CR2032) were assembled in a glovebox (Mbraun, USA) under a controlled environment with high purity argon gas. Glass microfibers were used as the separator (9934-AH, Whatman Glass microfibers). In 1 M LiPF₆ solution in ethylene carbonate (EC)/dimethyl carbonate (DMC) (1:1 v/v) was prepared and used as the electrolyte. Cyclic voltammetry (BSC-810 Bio-logic, France) was performed on the Li-ion half cells at a rate of 0.1 mV s⁻¹ between 0 and 3 V. Galvanostatic charge/discharge experiments were conducted under a current of 100 mA g⁻¹ from 0.05 to 3.0 V (CT2001A Landt, China). The rate performance was evaluated at current densities of 50, 100, 200, 400, 500, and 50 mA g⁻¹ (BT 2000 Arbin, US).

3 | RESULTS AND DISCUSSION

3.1 | Morphology and fiber formation

Figure 1 shows the fibers during centrifugal spinning as well as their appearance when collected, annealed, and carbonized. Among the three different PVP concentrations, the 25 wt% solution had the highest production yield of PVP fibers (Figure 1(a)). In previous studies, centrifugal spinning of PVP precursor solutions in ethanol with concentrations less than 20 wt%

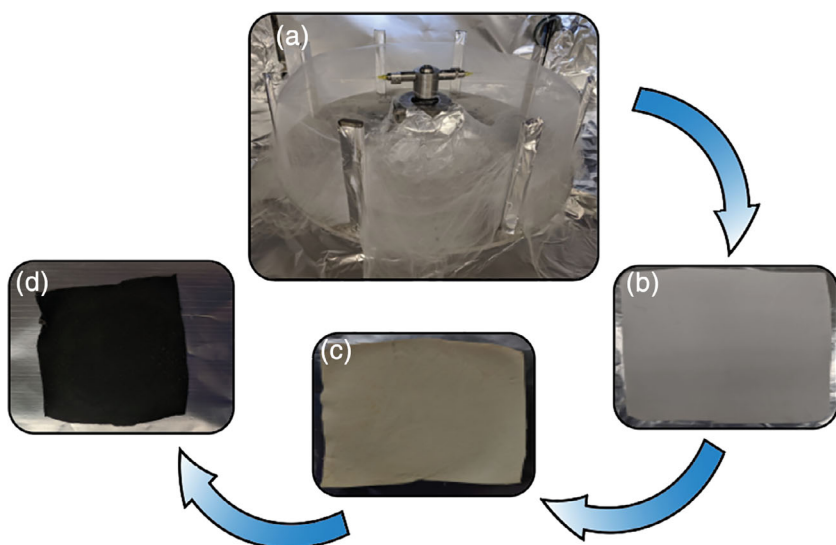


FIGURE 1 (a) Centrifugal spinning setup, (b) pristine collected fiber membrane, (c) annealed fiber membrane, and (d) carbonized fibers [Color figure can be viewed at wileyonlinelibrary.com]

resulted in bead-free PVP nanofibers with a high yield^{17,18}. When using water as the solvent, PVP fibers were only produced with polymer concentrations of 20 wt% or higher. At 25 wt%, the fiber production rate from an aqueous PVP solution was able to match that from PVP/ethanol precursor solutions. The 20 wt% PVP solution also produced similar amounts, but at this concentration the production of fibers became more sensitive to higher values of humidity, whereas the 25 and 28 wt% solutions were unaffected by the humidity. Although the 28 wt% PVP solution was not as sensitive to humidity, it yielded lower amounts of beaded fibers. It has been hypothesized that solvents with higher volatility lead to higher viscosity during the fiber formation in centrifugal spinning.²⁴ The faster vaporization rate of ethanol leads to a higher viscosity at the tip of the needle before producing a fiber jet. Thus, to compensate for the lower vapor pressure of water, higher polymer concentrations are needed to increase the viscosity of the solution.²⁴ Also, the fiber yield increased with increasing spinneret rotational speed, which caused an increase in the solvent evaporation rate.

The fibrous mats retained a similar overall volume and surface area after annealing, but their appearance, weight, and average fiber diameter changed. The fibers turned from white to a yellow color and an average of 21.3% weight loss was measured after annealing. This is attributed to the excess water in the fibers that evaporated during the heat treatment. After carbonization, the fibers suffered an average of 63.2% weight loss. Although the fibers shrank after the carbonization process, they remained flexible. The fiber flexibility allows the CFs to be used as binder-free anodes in LIBs. Moreover, these flexible fibers were achieved at a

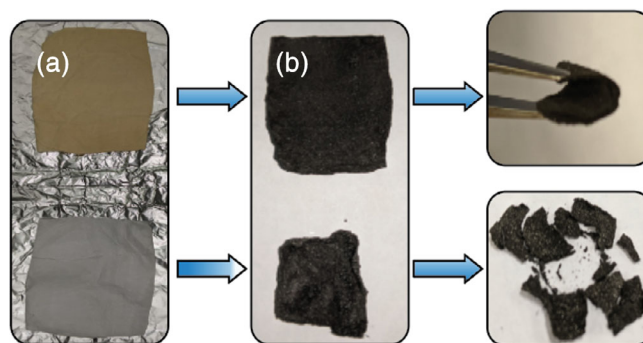


FIGURE 2 (a) Pristine (bottom) and annealed (top) fibrous membranes, (b) carbonized fibers from pristine (bottom) and annealed (top) fibrous membranes [Color figure can be viewed at wileyonlinelibrary.com]

higher carbonization temperature than that in similar studies.^{2,17,18}

In order to compare the structure of the CFs obtained from annealed and pristine fibers; both PVP precursor fibers were oxidized and then carbonized using the above-mentioned heat treatment. This comparison corroborated that the annealing process is crucial to produce flexible CFs. Figure 2 shows the pristine (bottom) and annealed (top) fibers before carbonization and the resultant structure. As shown in Figure 2, when the carbonization of PVP fibers was performed without the annealing process, brittle carbon fibers were obtained. On the other hand, the annealed fibers yielded a higher amount of carbon with a flexible structure.

In order to investigate the morphology and determine the average diameter of the fibers, SEM images were taken at a constant magnification of 1000X. Figure 3 shows the average diameter of the pristine, annealed, and

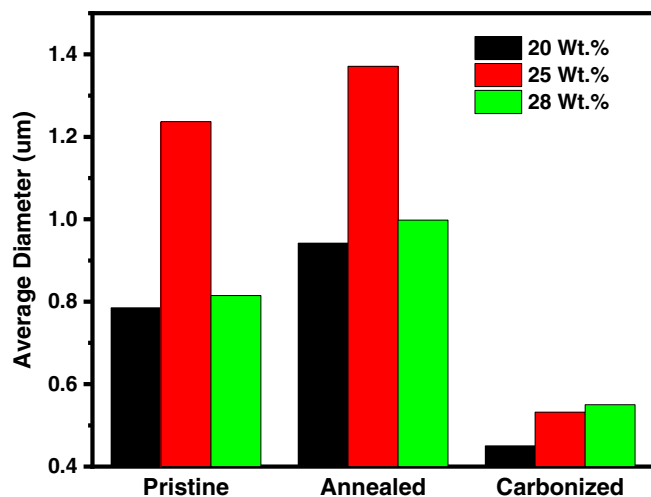


FIGURE 3 Average diameters of pristine, annealed, and carbonized fibers prepared from the 20, 25, and 28 wt% PVP aqueous solutions. PVP, poly(vinylpyrrolidone) [Color figure can be viewed at wileyonlinelibrary.com]

carbonized fibers prepared from PVP precursor solutions with different concentrations of 20, 25, and 28 wt%. Figures 4(a),(b),(c) show the SEM images and diameter distribution (histograms) of the pristine, annealed, and carbonized fibers prepared from the 20, 25, and 28 wt% PVP solutions, respectively. A common behavior observed is that the annealing process resulted in increased diameters of the pristine fibers. For the 28 wt% PVP fibers, one can observe that the fiber diameter not only increased, but a significant change in morphology also took place. The pristine 28 wt% PVP fibers had a “ramen-like” structure, but their morphology changed to a more homogeneous cylindrical shape due to the reduction of residual stresses after the annealing process. Another observation is that beads are less present in fibers prepared from the 20 and 25 wt% PVP solutions. This can be attributed to the lower vapor pressure in more concentrated aqueous PVP solutions, since the longer evaporation time of the more concentrated solutions allows for the formation of spheres due to Rayleigh instabilities during the jet formation in centrifugal spinning.²⁴

The SEM images of Figure 4(a), d, and (g) show that the number of beads in the pristine fibers increased with increasing polymer concentration. Moreover, the 20 and 25 wt% PVP solutions (Figure 4(a),(d)) exhibited a cylindrical fiber cross-section while the 28 wt% PVP fibers (Figure 4(g)) had an oval cross-section, with signs of residual surface tension during fiber formation. The production rate was similar for the pristine fibers prepared from the 20 and 28 wt% PVP precursor solutions. Also, the pristine fibers had average diameters that only varied by 0.08 µm. On the other hand, a much higher fiber

production rate was achieved using the 25 wt% PVP precursor solution (Figure 4(d)). However, these pristine fibers had a larger average diameter of 1.24 µm.

After annealing, the average diameter of all the PVP fibers increased (Figure 4(b), (e), and (h)). The average diameter of the annealed 20 and 28 wt% PVP fibers remained relatively closed to each other (0.94 and 1.00 µm) while the average diameter of the annealed 25 wt% PVP fibers was higher (1.37 m). More importantly, a change in morphology was observed in the 28 wt% PVP fibers during annealing. The oval cross-section became circular and the residual surface tension was reduced. Thus, cylindrical PVP fibers with a smooth surface were obtained after annealing. After carbonization, the 20, 25, and 28 wt% PVP derived carbon fibers (Figures 4(c),(f),(i)) had cylindrical shapes. However, the average diameter increased with increasing polymer concentration (Figure 3).

3.2 | Raman spectroscopy

The Raman lines of PVP powder and the corresponding centrifugally spun nanofibers are shown in Figure 5. It is observed that there are no significant differences among the Raman spectra, with the exception of an isolated, weak, and narrow line located at about 2300 cm⁻¹. This line may reflect a strong hydrogen bonding or C=O stretching.²⁵

The Raman spectra of the centrifugally spun PVP nanofibers were not significantly affected by the polymer concentration. The fact that the Raman spectrum is not significantly affected by the centrifugal spinning process is reasonable as the size of the nanofibers was not sufficiently small to ignite confinement effects.

In the low Raman shift regions, relatively few broad lines were recorded in the pristine and annealed PVP fibers at 133, 365, and 556 cm⁻¹. They are tentatively assigned to longitudinal acoustic modes or ring vibrations. C-C ring vibrations and breathing modes were reported at 760 and 937 cm⁻¹, respectively.^{26,27}

As shown in Figure 8, the carbonization process of the PVP nanofibers at 700 °C produced substantial changes in the Raman spectra of the nanofibers. Most of the lines assigned to PVP powder or nanofibers are completely erased by the carbonization process. Apparently, only the line located at 1235 cm⁻¹ survived, although it is slightly shifted and broadened. The most intense line located at 1363 cm⁻¹ was identified as the D band in carbonaceous materials.²⁸ The G line is located at about 1568 cm⁻¹,²⁸ being weak and broad and appears as a shoulder of the D band. Furthermore, the line observed at 1874 cm⁻¹ was tentatively assigned to C=O bonds, reflecting the oxidation of the polymer chains,

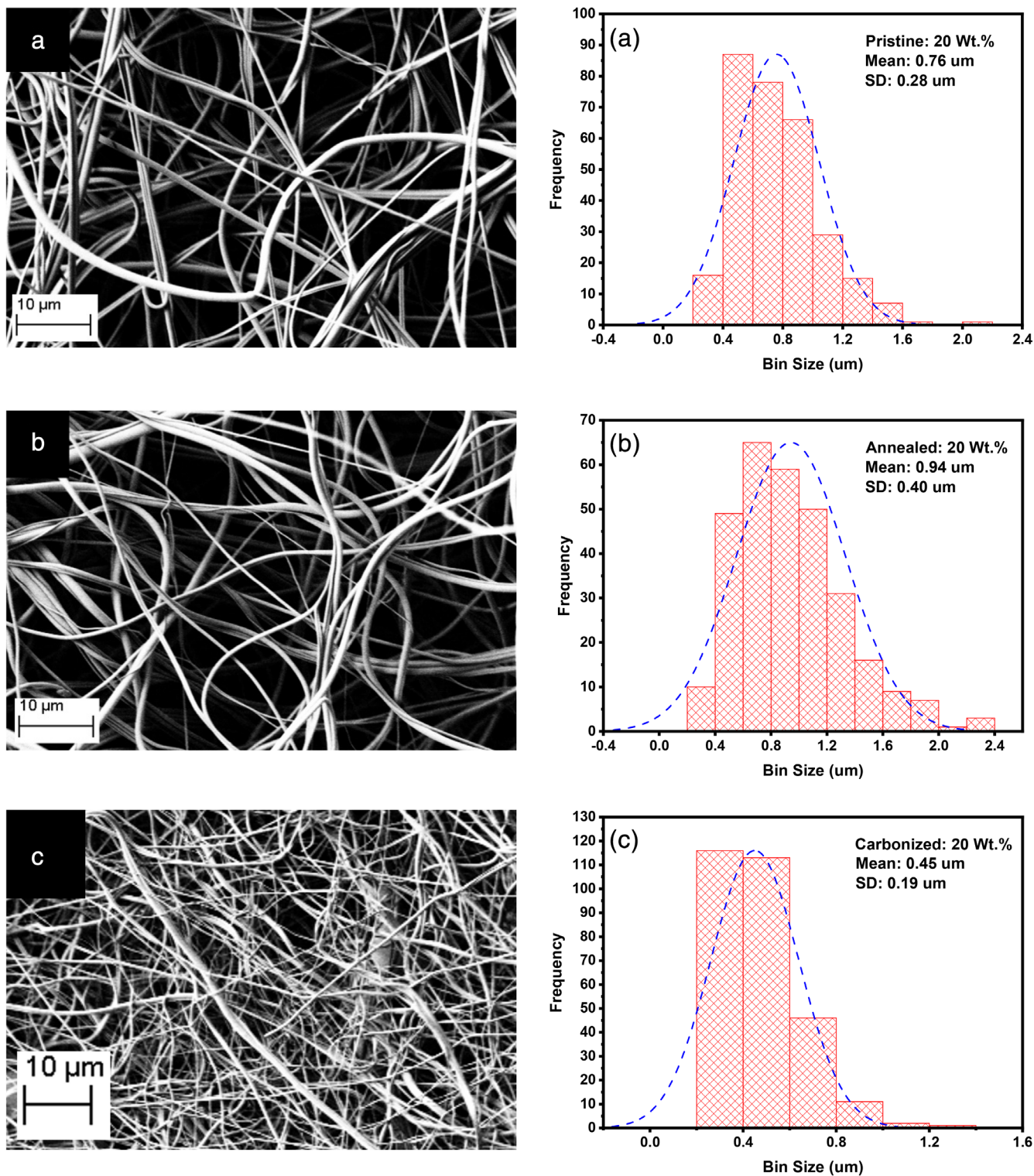


FIGURE 4 SEM images of fibers prepared from PVP solutions: (a) pristine, (b) annealed, and (c) carbonized fibers from 20 wt% PVP precursor solutions; (d) pristine, (e) annealed, and (f) carbonized fibers from 25 wt% PVP precursor solutions; (g) pristine, (h) annealed, and (i) carbonized fibers from 28 wt% PVP precursor solutions. PVP, poly(vinylpyrrolidone); SEM, scanning electron microscopy [Color figure can be viewed at wileyonlinelibrary.com]

while the line at 2368 cm^{-1} was identified as G' (i.e., as an overtone 2 phonon process) of the D band.²⁸ Finally, the line at 3269 cm^{-1} may be assigned as an overtone of the G

band.^{28,29} Thus, the carbonization process of the PVP nanofibers resulted into the appearance of the D and G bands, a feature that was reported in a previous study.³⁰

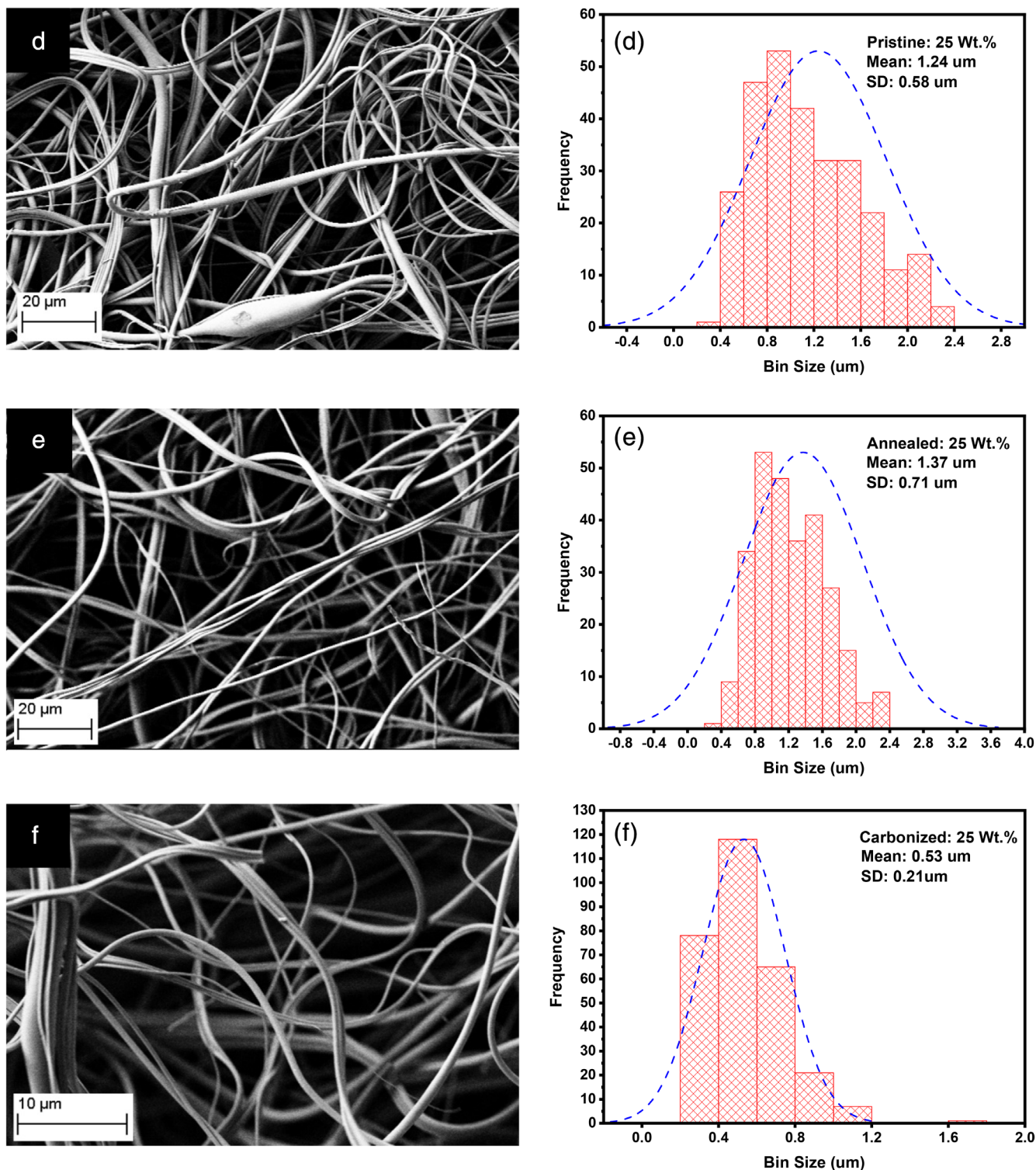


FIGURE 4 (Continued)

Figure 6(a),(b) show the effect of the annealing at 150°C on the PVP nanofibers obtained from the 20% PVP solution. A detailed analysis showed that the main consequences of the annealing process were manifested by a decrease of the amplitude of the Raman lines and their broadening. It was noticed that within

experimental errors, the line positions were not significantly affected by annealing and that all intense lines were still present in the spectrum of the annealed nanofiber. A similar behavior was observed for the annealed nanofibers obtained from 25% and 28% PVP solutions.

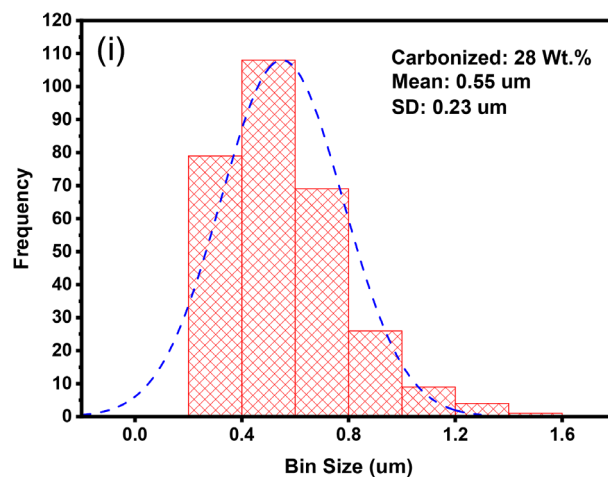
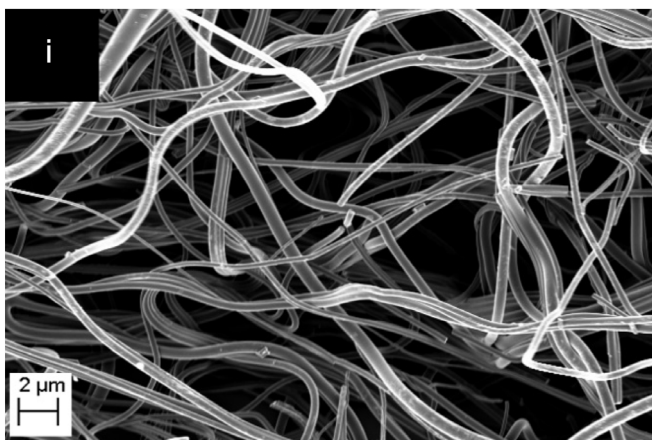
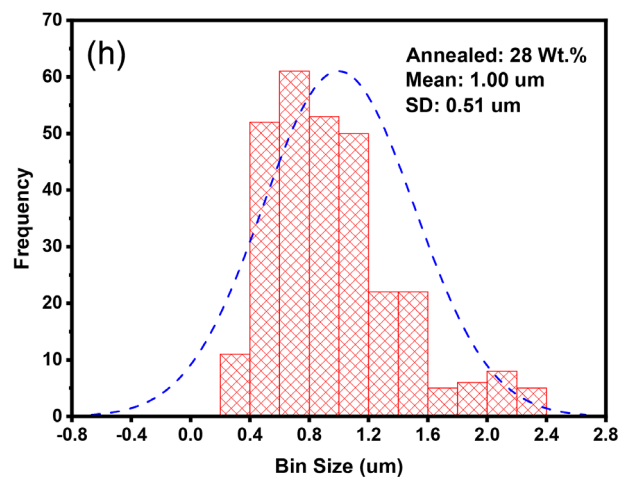
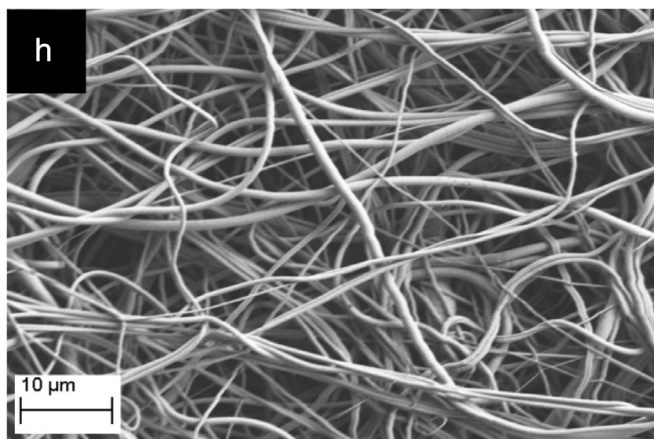
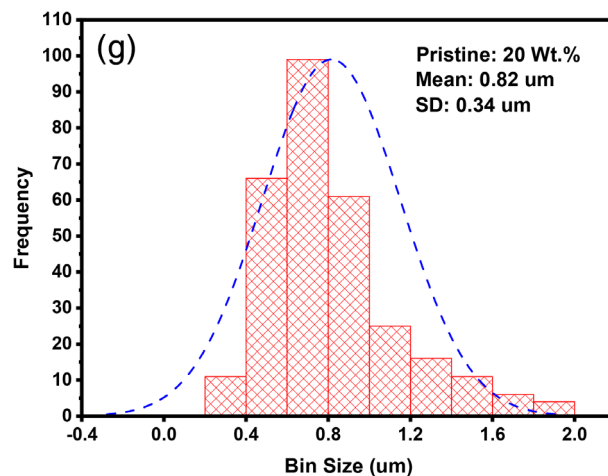
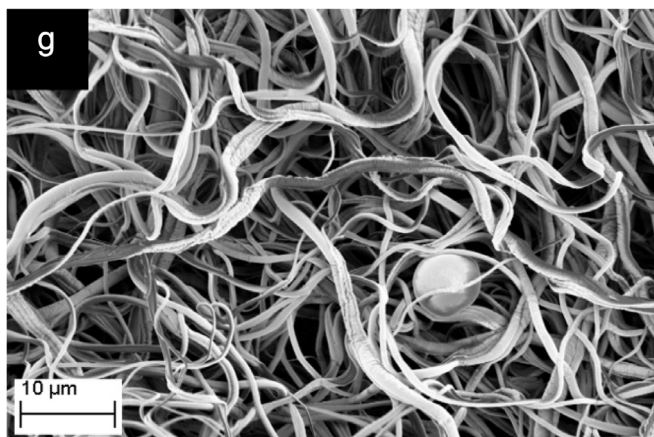


FIGURE 4 (Continued)

Figure 7 shows the Raman spectra of the PVP powder and the corresponding pristine, annealed and carbonized nanofibers obtained from a solution containing 20 wt% PVP in water. The annealing process of the PVP nanofibers decreased drastically the intensity of the Raman lines while very large modifications were noticed in the carbonized sample.

3.3 | Thermogravimetric analysis

TGA was conducted on pristine and annealed PVP fibers in air and nitrogen atmospheres to assess the resilience of annealed fibers to degradation. In this analysis, a heating rate of 5°C/min was used for all the samples in a range between 25 and 700°C. In both air and nitrogen

atmospheres the annealed fibers yielded more residue than the pristine fibers. The residual masses for both samples are illustrated in Figure 8. Under an airflow, the annealed fibers yielded a residual mass of 3% while the pristine fibers only yielded a 0.6% residual mass. Thus, the annealed PVP fibers produced about five times more residue than the pristine PVP fibers. When both annealed and pristine fibers were heated in an inert flow (nitrogen), the annealed fibers yielded a residual mass of 11.3% while the pristine fibers yielded 5.4%. In this case, the annealed fibers produced twice the amount of residue produced by the pristine fibers, indicating that the carbon yield in the annealed fibers is higher. This comparison

shows that, indeed, annealed fibers have a higher resistance to degradation. Even though both annealed and pristine fibers reached a degradation plateau at the same temperature ($\sim 450^\circ\text{C}$ under nitrogen and $\sim 650^\circ\text{C}$ in air), the lower degradation rate in the annealed fibers enabled them to retain more carbon when their respective degradation threshold temperature was reached. Nevertheless, it is crucial to mention that these residual mass percentages are based on the initial mass (100%) of the fibers at room temperature. In Figure 8, an initial mass drop was observed in both air and nitrogen atmospheres at temperatures below the onset of degradation. This initial mass loss is attributed to the evaporation of water absorbed by the PVP fibers, which is hydrophilic. This is supported by Raman spectra, which did not reveal the disappearance (or appearance of new) Raman lines upon annealing. Thus, using the first plateau as the reference of 100% weight, higher percentages of carbon yield for both the pristine and annealed PVP fibers can be determined. Using the TGA data analyzer software (TG 209 F3 Tarsus, NETZSCH, Germany), the mass changes between the first and second plateaus were determined as -63.9% and -73.6% for the annealed and pristine fibers, respectively. Thus, residual masses of 36.1% and 26.5% can be obtained (Figure 9) for the annealed and pristine fibers, respectively. These values are congruous with the average mass losses weighed from the annealed fibers before and after carbonization (63.2 wt%). Based on the EDS analysis performed on the residues obtained from annealed and pristine fibers under nitrogen, the annealed fibers yielded 85% carbon out of its TGA residue, while the pristine fibers yielded 89% carbon. Thus, using these adjusted values, the annealed PVP fibers yielded 30.6% carbon while the pristine PVP fibers yielded 23.1% carbon.

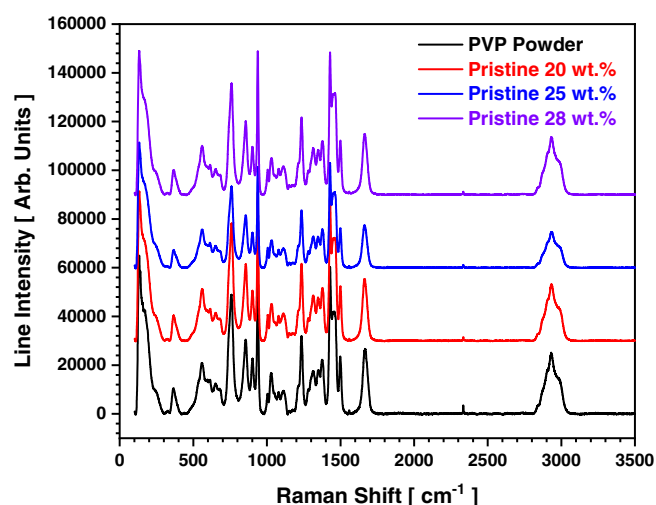


FIGURE 5 Raman lines of PVP powder and PVP pristine fibers prepared from solutions with PVP concentrations of 20, 25, and 28 wt%. PVP, poly(vinylpyrrolidone) [Color figure can be viewed at wileyonlinelibrary.com]

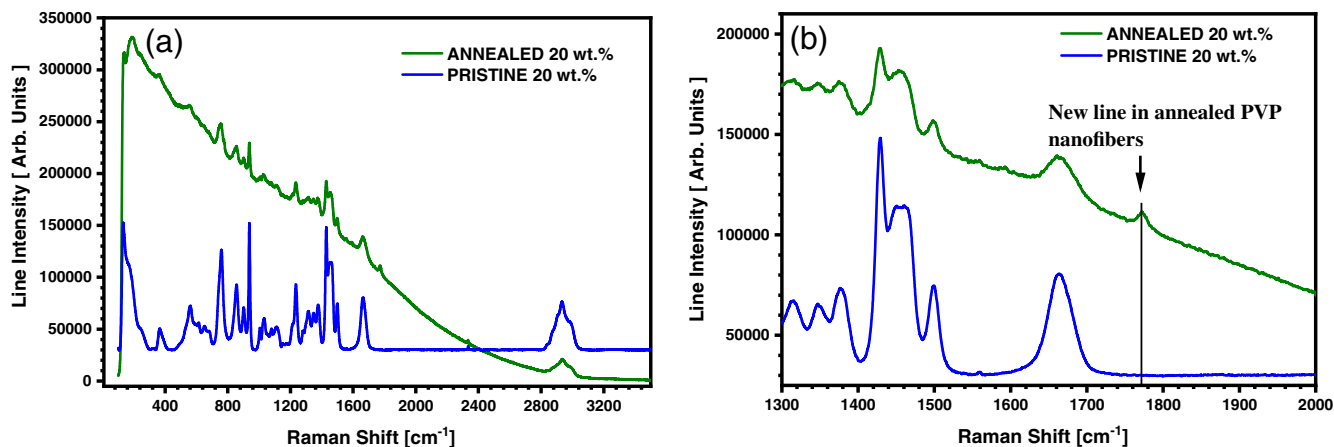


FIGURE 6 A comparison between the Raman spectra of pristine and annealed fibers prepared from the 20 wt% PVP solution in water. PVP, poly(vinylpyrrolidone) [Color figure can be viewed at wileyonlinelibrary.com]

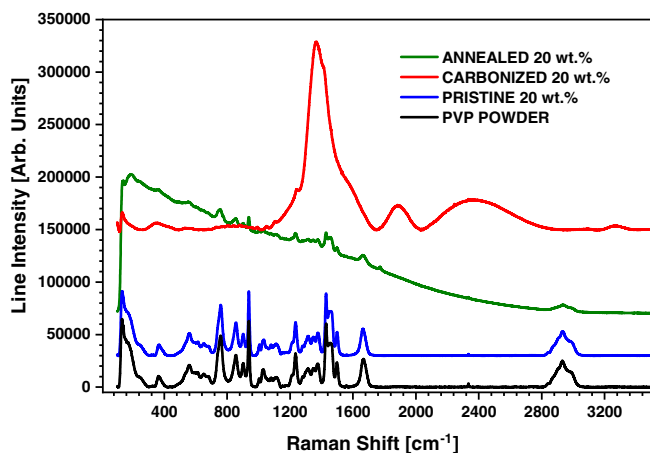


FIGURE 7 Raman spectra of PVP powder, and PVP pristine, annealed, and carbonized fibers prepared from the 20 wt% solution. PVP, poly(vinylpyrrolidone) [Color figure can be viewed at wileyonlinelibrary.com]

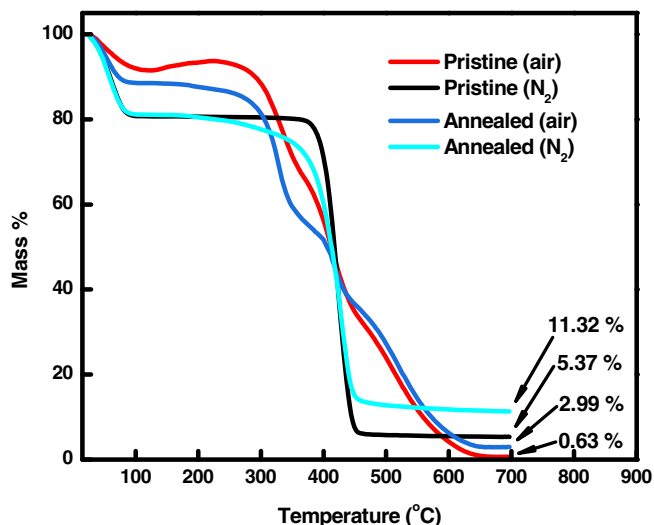


FIGURE 8 TGA analysis of the pristine and annealed PVP fibers in air and nitrogen atmospheres. PVP, poly(vinylpyrrolidone); TGA, thermogravimetric analysis [Color figure can be viewed at wileyonlinelibrary.com]

3.4 | Electrochemical performance of carbon-fiber anodes

3.4.1 | Cyclic voltammetry

Cyclic voltammetry (CV) tests were performed on carbon-fiber anodes prepared from PVP precursor solutions with 20, 25, and 28 wt% concentrations. Figure 10 shows the CV scans of the 25 wt% derived carbon fibers. The CV results for the other two compositions of CFs are shown in Figures S1 and S2 of the supplementary information (SI). For all three carbon-fiber anodes, a broad

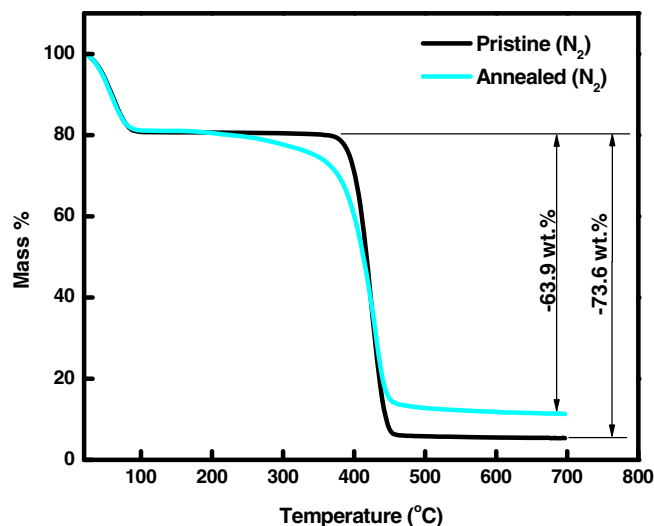


FIGURE 9 Mass loss percentage after removal of water from the pristine and annealed fibers in a nitrogen atmosphere [Color figure can be viewed at wileyonlinelibrary.com]

anode reduction peak was observed at ~ 0.1 V during the cathodic scan. Wide anode oxidation peaks during the anodic scans appeared in all three anodes due to ion de-intercalation at ~ 0.5 V and ~ 1.5 V. These anode oxidation peaks represent the working voltage of the anode as well as the solid electrolyte interphase (SEI) formation voltage due to Li^+ de-intercalation during the first cycle.³¹

3.4.2 | Cycle performance

The charge/discharge profiles of the carbon-fiber anodes, prepared from PVP concentration of 25 wt%, are shown in Figure 11. The charge discharge plots and cycle performance for the CF anodes prepared from PVP precursor fibers with PVP concentrations of 20 and 28 wt%, are shown in Figure S3. The galvanostatic charge/discharge experiments were performed at a current density of 100 mA g^{-1} . At the 1st cycle, the 20, 25, and 28 wt% PVP-derived carbon fibers delivered a charge capacity of 205, 189, and 275 mAh g^{-1} , respectively. After the first cycle, the CF anodes maintained a consistent capacity and after 100 cycles, the 20, 25, and 28 wt% PVP-derived carbon fiber anodes delivered charge capacities of 185, 194, and 214 mAh g^{-1} , respectively.

The high irreversible capacity at the first cycle is caused by the decomposition of the electrolyte that leads to the formation of an irreversible solid electrolyte interphase (SEI) layer on the surface of the carbon-fiber anode and, consequently, results in a low initial Coulombic efficiency.^{32,33} The high surface area of the fibers can also

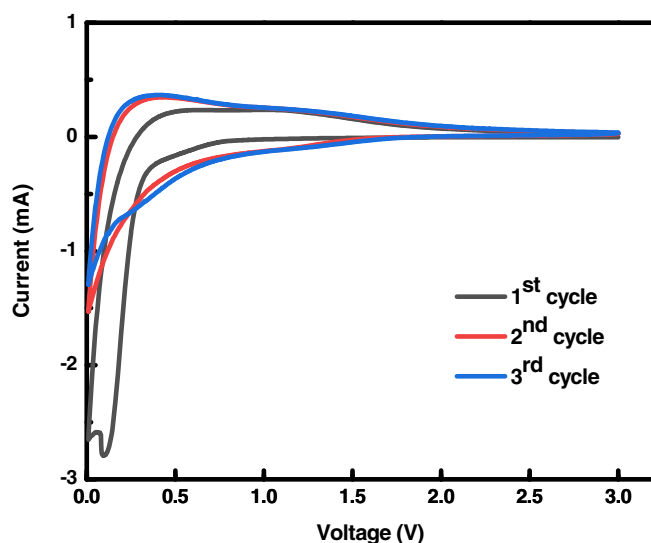


FIGURE 10 Cycle voltammetry of carbon fibers prepared from PVP precursor fibers with PVP concentration of 25 wt%. PVP, poly(vinylpyrrolidone) [Color figure can be viewed at wileyonlinelibrary.com]

contribute to the low initial Coulombic efficiency of the anode. In fact, the large surface area of the nanofibers can lead to the formation of a thicker (larger) SEI layer at the first cycle compared to slurry-based carbon electrodes.³⁴ Results reported on centrifugally spun carbon and composite fibers as anodes for Li-ion and Na-ion batteries showed also low initial Coulombic efficiency.^{34,35}

Figure 12 shows the charge capacities of the three anodes after 100 cycles at 100 mA g^{-1} . The large drop in capacity after the first cycle can be attributed to the high surface area of the fibers and the growth of the solid electric interphase (SEI) layer on the electrode. As a result, the coulombic efficiency at the first cycle for the 20, 25, and 28 wt% was 39.8, 34.2, and 44.4%, and after 100 cycles, the coulombic efficiency reached 99.6, 99.3, and 99.6%, respectively.

3.5 | Rate performance

Figure 13 shows the rate performance of the 20, 25, and 28 wt% PVP-based anodes at different current densities of 50, 100, 200, 400, and 500 mA h g^{-1} in a voltage range between 0.01 and 3.0 V. The charge capacity decreases as the current rate increases due to the faster rates of lithiation/delithiation that overwhelm the pace of insertion/deinsertion of Li-ions into the electrodes. It is also observed that the specific capacity at higher current rates decreases more rapidly for the carbon fibers anodes made prepared from PVP solutions with higher concentration; this can be attributed to the larger fiber diameter. In

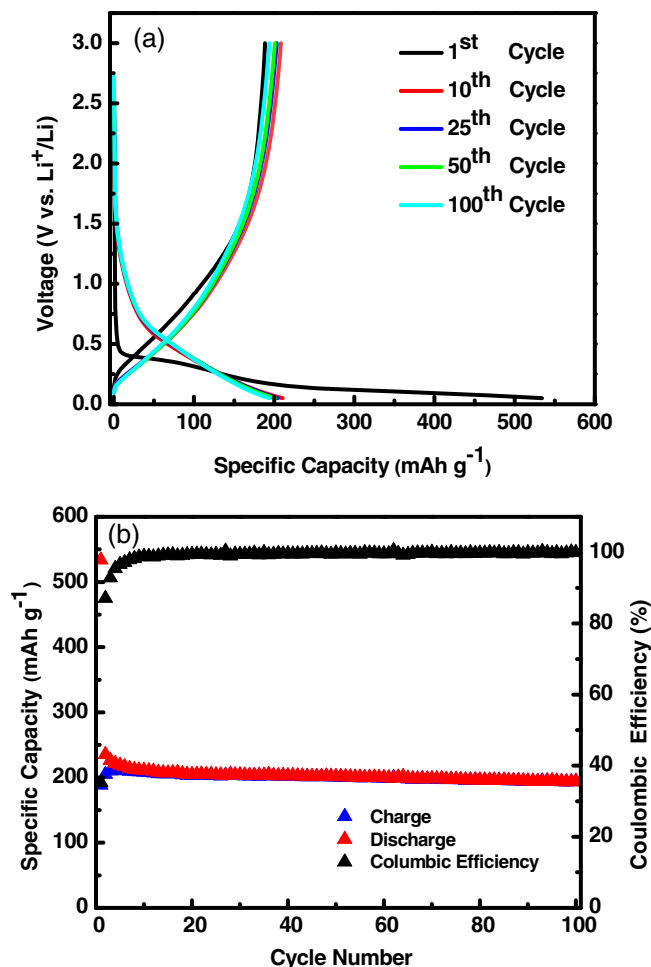


FIGURE 11 (a) Galvanostatic charge-discharge curves and (b) cycle performance and coulombic efficiency of carbon fibers prepared from precursor fibers with 25 wt% PVP concentration. PVP, poly(vinylpyrrolidone) [Color figure can be viewed at wileyonlinelibrary.com]

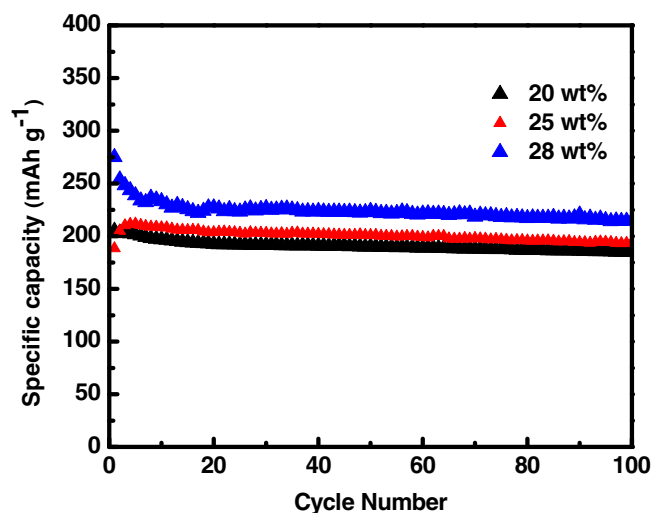


FIGURE 12 Specific charge capacity for the 20, 25, and 28 wt% derived carbon fibers [Color figure can be viewed at wileyonlinelibrary.com]

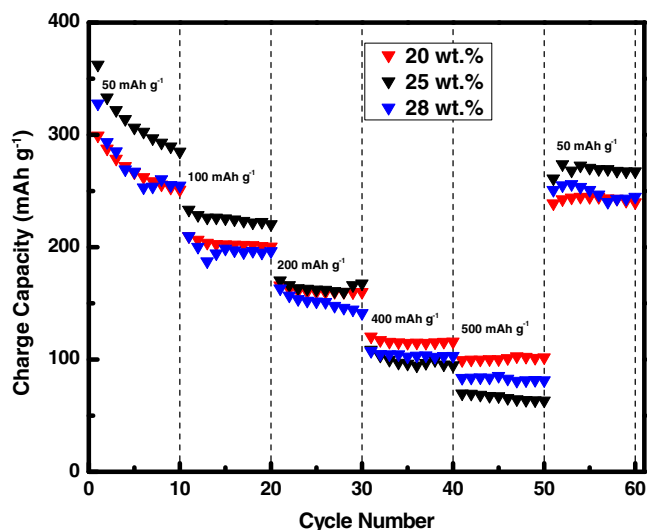


FIGURE 13 Rate performance for the 20, 25 and 28 wt% PVP derived anodes. PVP, poly(vinylpyrrolidone) [Color figure can be viewed at wileyonlinelibrary.com]

these anodes, the larger fiber diameters become a bottleneck during faster rates due to less available surface area for lithiation. Nonetheless, after cycling back to 50 mA g⁻¹, the 20, 25, and 28 wt% derived carbon-fiber anodes recovered ~96.9, ~94.2, and ~96.9% of their initial capacity during the first 10 cycles at 50 mA h g⁻¹. Moreover, the anodes also delivered a constant capacity at each current rate. This is expected since there is not an added active material that could produce anode pulverization after cycling caused by excessive volume change.

4 | CONCLUSIONS

In this work, a higher rate of carbon nanofibers from aqueous PVP solutions was achieved using centrifugal spinning and subsequent thermal treatment. Solutions with PVP concentrations of 10, 15, 20, 25, and 28 wt% were prepared, of which only the 20, 25, and 28 wt% produced fibers. Although beads were less apparent in lower concentration solutions, the highest fiber yield was possible at 25 wt% PVP. Moreover, at this concentration, the fiber formation was not affected by higher humidity levels. Flexible carbon fibers were produced using the 20, 25, and 28 wt% PVP precursor fibers using a novel three-step heat treatment which reduced the volume shrinkage of fibers due to the high temperature (700°C) used during the carbonization process. The electrochemical results were similar for all carbon fibers. Two trends were observed during the cycle and rate performances. First, the specific capacity increased with increasing PVP

concentration in water solutions; more work is needed to understand the effect of polymer concentration on the electrochemical performance of PVP derived carbon fiber anodes. Second, during the rate performance tests, the higher polymer concentration resulted in a lower specific capacity at a faster charge/discharge rate. This might be attributed to the increase in fiber CFs diameter of the 25 and 28 wt% derived anodes. Given these results, a new venue to produce binder-free carbon composite anodes from aqueous polymer solutions at a larger scale can be pursued to reduce the environmental impact and the health risks encountered during the production of fibers from polymer solutions in toxic solvents. Moreover, this work lay the foundation for the development of high rate composite nanofibers production using water as the sole solvent.

ACKNOWLEDGMENT

This research was supported by NSF PREM award under grant No. DMR-1523577: UTRGV-UMN Partnership for Fostering Innovation by Bridging Excellence in Research and Student Success. Part of this work was carried out in the College of Science and Engineering Characterization Facility, University of Minnesota, which has received capital equipment funding from the NSF through the UMN MRSEC program under Award Number DMR-1420013.

REFERENCES

- [1] M. Ramalingam, S. Ramakrishna, *Nanofiber Composites for Biomedical Applications*, Elsevier, Amsterdam, Netherlands **2017**, p. Xvii.
- [2] L. Zuniga, G. Gonzalez, R. O. Chavez, J. C. Myers, T. P. Lodge, M. Alcoutlabi, *Appl. Sci. Basel* **2019**, *9*, ARTN 4032.
- [3] D. De la Garza, F. De Santiago, L. Materon, M. Chipara, M. Alcoutlabi, *J. Appl. Polym. Sci.* **2019**, *136*, ARTN 47480.
- [4] V. Lukasova, M. Buzgo, K. Vocetkova, V. Sovkova, M. Doupnik, E. Himawan, A. Staffa, R. Sedlacek, H. Chlup, F. Rustichelli, E. Amler, M. Rampichova, *Mater. Sci. Eng. C-Mater. Biol. Appl.* **2019**, *97*, 567.
- [5] Calisir, M.D. and Kilic, A., 'A Comparative Study on SiO₂ Nanofiber Production Via Two Novel Non-Electrospinning Methods: Centrifugal Spinning Vs Solution Blowing', *Materials Letters*, **2020**, 258 ARTN 126751,
- [6] B. A. Zhang, F. Y. Kang, J. M. Tarascon, J. K. Kim, *Prog. Mater. Sci.* **2016**, *76*, 319.
- [7] L. W. Ji, Z. Lin, M. Alcoutlabi, X. W. Zhang, *Energy Environ. Sci.* **2011**, *4*, 2682.
- [8] C. Kim, K. S. Yang, M. Kojima, K. Yoshida, Y. J. Kim, Y. A. Kim, M. Endo, *Adv. Funct. Mater.* **2006**, *16*, 2393.
- [9] M. Zhang, J. Wang, S. Chen, F. Wu, *Proc. 3rd Int. Conf. Mater. Eng. Appl. (Icmea)* **2016**, 2016, 380.
- [10] P. Q. Wang, D. Zhang, F. Y. Ma, Y. Ou, Q. N. Chen, S. H. Xie, J. Y. Li, *Nanoscale* **2012**, *4*, 7199.
- [11] L. T. Dong, G. W. Wang, X. F. Li, D. B. Xiong, B. Yan, B. X. Chen, D. J. Li, Y. H. Cui, *RSC Adv.* **2016**, *6*, 4193.

- [12] V. A. Agubra, L. Zuniga, D. Garza, L. Gallegos, M. Pokhrel, M. Alcoutlabi, *Solid State Ionics* **2016**, 286, 72.
- [13] Lopez, J., Gonzalez, R., Ayala, J., Cantu, J., Castillo, A., Parsons, J., Myers, J., Lodge, T.P., Alcoutlabi, M.J.J.o.P., and Solids, C.o., 'Centrifugally Spun Tio₂/C Composite Fibers Prepared from Tis₂/Pan Precursor Fibers as Binder-Free Anodes for Libs', 2021, 149, p. 109795
- [14] J. Spender, A. L. Demers, X. F. Xie, A. E. Cline, M. A. Earle, L. D. Ellis, D. J. Neivandt, *Nano Lett.* **2012**, 12, 3857.
- [15] L. Fei, B. P. Williams, S. H. Yoo, J. Kim, G. Shoorideh, Y. L. Joo, in *Acs Appl. Mater. Interfaces*, Vol. 8 **2016**, p. 5243.
- [16] R. Nava, L. Cremar, V. Agubra, J. Sanchez, M. Alcoutlabi, K. Lozano, *ACS Appl. Mater. Interfaces* **2016**, 8, 29365.
- [17] L. Zuniga, V. Agubra, D. Flores, H. Campos, J. Villareal, M. Alcoutlabi, *J. Alloys Compd.* **2016**, 686, 733.
- [18] D. Flores, J. Villarreal, J. Lopez, M. Alcoutlabi, *Materials Science and Engineering B-Advanced Functional Solid-State Materials* **2018**, 236, 70.
- [19] Villarreal, J., Chavez, R.O., Chopade, S.A., Lodge, T.P., and Alcoutlabi, M., 'The Use of Succinonitrile as an Electrolyte Additive for Composite-Fiber Membranes in Lithium-Ion Batteries', *Membranes*, **2020**, 10, ARTN 45.
- [20] M. Akia, N. Salinas, S. Luna, E. Medina, A. Valdez, J. Lopez, J. Ayala, M. Alcoutlabi, K. Lozano, *J. Mater. Sci.* **2019**, 54, 13479.
- [21] Niu, H.T., Zhang, J., Xie, Z.L., Wang, X.G., and Lin, T., 'Preparation, Structure and Supercapacitance of Bonded Carbon Nanofiber Electrode Materials', *Carbon*, **2011**, 49, pp. 2380–2388.
- [22] I. M. Szilagyi, E. Santala, M. Heikkila, M. Kemell, T. Nikitin, L. Khriachtchev, M. Rasanen, M. Ritala, M. Leskela, *J. Therm. Anal. Calorim.* **2011**, 105, 73.
- [23] Z. McEachin, K. Lozano, *J. Appl. Polym. Sci.* **2012**, 126, 473.
- [24] H. M. Golecki, H. Y. Yuan, C. Glavin, B. Potter, M. R. Badrossamay, J. A. Goss, M. D. Phillips, K. K. Parker, *Langmuir* **2014**, 30, 13369.
- [25] P. Larkin, *Infrared and Raman Spectroscopy: Principles and Spectral Interpretation*, Elsevier, Amsterdam, Netherlands **2017**.
- [26] M. Dumitrascu, V. Meltzer, E. Sima, M. Virgolici, M. G. Albu, A. Fikai, V. Moise, R. Minea, C. Vancea, A. Scarisoreanu, F. Scarlat, *Digest Journal of Nanomaterials and Biostructures* **2011**, 6, 1793.
- [27] I. M. Alibe, K. A. Matori, H. A. Sidek, Y. Yaakob, U. Rashid, A. M. Alibe, M. H. M. Zaid, S. Nasir, M. M. Nasir, *J. Therm. Anal. Calorim.* **2019**, 136, 2249.
- [28] D. M. Chipara, A. C. Chipara, M. Chipara, *Spectroscopy* **2011**, 26, 42.
- [29] M. S. Dresselhaus, G. Dresselhaus, R. Saito, A. Jorio, *Physics Reports-Review Section of Physics Letters* **2005**, 409, 47.
- [30] O. Keri, P. Bardos, S. Boyadjiev, T. Igricz, Z. K. Nagy, I. M. Szilagyi, *J. Therm. Anal. Calorim.* **2019**, 137, 1249.
- [31] L. W. Ji, O. Toprakci, M. Alcoutlabi, Y. F. Yao, Y. Li, S. Zhang, B. K. Guo, Z. Lin, X. W. Zhang, *ACS Appl. Mater. Interfaces* **2012**, 4, 2672.
- [32] J. R. Dahn, T. Zheng, Y. H. Liu, J. S. Xue, *Science* **1995**, 270, 590.
- [33] Y. Tian, Y. L. An, C. L. Wei, B. J. Xi, S. L. L. Xiong, J. K. Feng, Y. T. Qian, *ACS Nano* **2019**, 13, 11676.
- [34] H. Jia, M. Dirican, C. Aksu, N. Sun, C. Chen, J. D. Zhu, P. Zhu, C. Y. Yan, Y. Li, Y. Q. Ge, J. S. Guo, X. W. Zhang, *J. Colloid Interface Sci.* **2019**, 536, 655.
- [35] J. D. Zhu, C. Chen, Y. Lu, Y. Q. Ge, H. Jiang, K. Fu, X. W. Zhang, *Carbon* **2015**, 94, 189.

SUPPORTING INFORMATION

Additional supporting information may be found online in the Supporting Information section at the end of this article.

How to cite this article: Chavez RO, Lodge TP, Huitron J, Chipara M, Alcoutlabi M. Centrifugally spun carbon fibers prepared from aqueous poly(vinylpyrrolidone) solutions as binder-free anodes in lithium-ion batteries. *J Appl Polym Sci.* 2021; 138:e50396. <https://doi.org/10.1002/app.50396>